Calculated de Haas-van Alphen quantities of CeMIn$_5$ (M =Co, Rh, and Ir) compounds

S. Elgazzar,[1,2] I. Opahle,[1] R. Hayn,[1,3] and P. M. Oppeneer[1,4]
[1] *Leibniz-Institute of Solid State and Materials Research, P.O. Box 270016, D-01171 Dresden, Germany*
[2] *Department of Physics, Faculty of Science, Menoufia University, Shebin El-kom, Egypt*
[3] *Laboratoire Matériaux et Microélectronique de Provence, Case 142, Université d'Aix-Marseille III, Faculté Saint-Jerôme, 13397 Marseille Cedex 20, France*
[4] *Department of Physics, Uppsala University, Box 530, S-751 21 Uppsala, Sweden*
(Dated: February 2, 2008)

We report a critical analysis of the electronic structures and de Haas-van Alphen (dHvA) quantities of the heavy-fermion superconductors $CeCoIn_5$, $CeRhIn_5$, and $CeIrIn_5$. The electronic structures are investigated *ab initio* on the basis of full-potential band-structure calculations, adopting both the scalar- and fully relativistic formulations within the framework of the local spin-density approximation (LSDA). In contrast to another recent study, in which a pronounced change of the Fermi surface due to relativistic effects and therefore the importance of relativistic interactions for the superconductivity was claimed, we find only minor relativistic modifications of the band structure in our calculations. The *ab initio* calculated dHvA quantities are in good agreement with experimental data for $CeCoIn_5$ and $CeIrIn_5$, when we adopt the delocalized LSDA description for the Ce $4f$ states. For $CeRhIn_5$, however, a better agreement with experiment is obtained when the Ce $4f$ electron is treated as a localized core electron. The implications for an emerging picture of the localization behavior of the $4f$ electron in these materials are discussed. We furthermore compare our calculated dHvA quantities with other recent relativistic calculations and discuss the differences between them.

PACS numbers: 78.20.-e, 71.20.-b, 71.28.+d

I. INTRODUCTION

A new group of fascinating heavy-fermion superconductors that crystallize in the $HoCoGa_5$ structure was discovered a few years ago.[1] To the superconductors of this group that have received wide attention belong $CeCoIn_5$, $CeRhIn_5$, and $CeIrIn_5$ (Refs. 1,2,3). $CeCoIn_5$ and $CeIrIn_5$ are superconductors at ambient pressure,[2,3] with $T_c = 0.4$ and 2.3 K, respectively, whereas $CeRhIn_5$ becomes a superconductor (with $T_c = 2.1$ K) under pressure.[1] At ambient pressure $CeRhIn_5$ orders antiferromagnetically with an incommensurate spin spiral below the Néel temperature $T_N = 3.9$ K (Ref. 4). The entanglement of heavy-fermion behavior, antiferromagnetism, and superconductivity seems to point to an unconventional pairing mechanism.[2,3] Unambiguous evidence for unconventional spin-singlet d-wave superconductivity in $CeRhIn_5$ and $CeCoIn_5$ was recently provided by a number of experiments.[5,6,7,8] The nature of the pairing mechanism, however, could not yet be established.

An important issue which has become intensively debated is the role of the Ce $4f$ electrons and their degree of localization. The high specific heat coefficients[2,3] of about 300 mJ/molK^2 to 750 mJ/molK^2 for $CeCoIn_5$ and $CeIrIn_5$, respectively, indicate at least some $4f$ delocalization at ambient pressure. The $4f$ localization has been studied in some detail by de Haas-van Alphen (dHvA) experiments,[9,10,11,12,13,14,15,16,17] in which especially $CeRhIn_5$ received attention.[9,10,11,12] Although the dHvA data of pure $CeRhIn_5$ were initially interpreted using an itinerant band-structure calculation with delocalized $4f$ electrons,[10] subsequent measurements of the dHvA quantities of $Ce_xLa_{1-x}RhIn_5$ indicated[11] that the Ce $4f$ electrons remain localized for all x. The rather low specific heat coefficient $\gamma \approx 50$ mJ/molK^2 at ambient pressure would corroborate localized $4f$ behavior in $CeRhIn_5$. Even in the localized picture, the $4f$ electrons are responsible for the magnetism which could, for example, through spin degrees of freedom, give rise to an unconventional pairing interaction.

De Haas-van Alphen measurements in connection with band-structure calculations are a very useful tool to analyze a multiband situation with a complicated Fermi surface. Such studies have been performed for the three Ce-115 compounds in question by several groups with contradictory results, however. In the case of $CeCoIn_5$, the authors of Ref. 13 found a reasonable agreement of the calculated dHvA data with the measured values,[12,13] having in their band structure three bands crossing the Fermi surface (see also Ref. 18). A similar agreement was found for the superconducting compound $CeIrIn_5$ (see Ref. 14). Conversely, another recent study[19] claimed an important influence of relativistic effects on the electronic structure of these two compounds, leading to a fourth band crossing the Fermi surface which would give rise to additional dHvA frequencies. If relativistic effects are important then this would obviously affect the microscopic understanding of the superconductivity (see, e.g., Ref. 20) and possibly of the pairing mechanism, which remains an unresolved issue. Another controversy was already noted and concerns $CeRhIn_5$ which is antiferromagnetic at ambient pressure. The authors of Ref. 10 interpreted its dHvA data by a nonmagnetic itinerant band structure calculation treating the $4f$ electrons as valence states and stating a reasonable agreement. On the contrary, the localized nature of the $4f$ electrons in

$CeRhIn_5$ was proposed in Ref. 15 on the basis of a comparison to the dHvA data of $LaRhIn_5$. Localization of the $4f$ electron was also revealed[11] by dHvA investigations of $Ce_xLa_{1-x}RhIn_5$, but no corresponding band-structure calculation was performed up to now.

Taking into account the apparent similarity within the electronic structure of all three compounds, a comparative and critical analysis of the electronic structures and de Haas-van Alphen quantities is highly desirable. Also, performing a complete theoretical analysis of the dHvA data for $H \parallel c$ of the three Ce-115 compounds using the same numerical method (as will be presented here) allows one to critically assess the reliability of former calculations. Comparing scalar-relativistic and fully relativistic calculations will answer the discussion concerning the importance of relativistic contributions, started in Ref. 19. In addition, comparing the Co-, Ir-compounds on one side with the Rh-compound on the other side (treating the $4f$ electron as core electron or not) may possibly prove whether the $4f$ electrons are localized or not.

For our study we use the full potential local orbital (FPLO) method[21,22] for all three compounds $CeCoIn_5$, $CeRhIn_5$, and $CeIrIn_5$. We calculate the extremal Fermi surface cross sections and effective masses and restrict ourselves to $H \parallel c$ for which most experimental data exist. We compare scalar-relativistic and fully relativistic calculations, and, in the case of $CeRhIn_5$, the localized and the delocalized descriptions of Ce $4f$ electrons. After presenting our method (Sec. II) and a short discussion of the resulting band structures (Sec. III) we describe the extremal orbits in Sec. IV. The critical comparison with former calculations and experimental results (Sec. V) allows to draw our conclusions in Sec. VI.

II. COMPUTATIONAL METHOD

We performed band-structure calculations using both the scalar-relativistic and the fully relativistic versions of the full potential local orbital minimum-basis band-structure method.[21,22] In these calculations, the following basis sets were adopted for the valence states: the $4f; 5s5p5d; 6s6p$ states for Ce when the $4f$ are treated as valence states, while for Co, Rh, Ir and In were used $3s3p3d; 4s4p$, $4s4p4d; 5s5p$, $5s5p5d; 6s6p$ and $4d; 5s5p$ respectively. The high lying $5s$ and $5p$ semicore states of Ce, which might hybridize with the $5d$ valence states, are thus included in the basis. The compression parameters x_0 were optimized for each basis orbital separately by minimizing the total energy. For the site-centered potentials and densities we used expansions in spherical harmonics up to l_{max}=12. The number of k-points in the irreducible part of Brillouin zone was 726, but some pivotal calculations were made also with higher numbers of k-points. The Perdew-Wang[23] parameterization of the exchange-correlation potential in the local spin-density approximation (LSDA) was used.

The dHvA cyclotron frequency F—which is proportional to the Fermi surface cross section—and the cyclotron mass m of the extremal orbits are calculated numerically by discretizing the Fermi velocities on k-points along the orbit and by a subsequent Romberg integration.[24]

III. BAND STRUCTURE

The compounds $CeMIn_5$ (M=Co, Rh, and Ir) crystallize in the tetragonal structure, space group P4/mmm (space group number 123) and are built of alternating stacks of $CeIn_3$ and MIn_2. We performed nonmagnetic band structure calculations for the experimental lattice parameters, which are (in atomic units): $a = 8.714\ a_0$ and $c = 14.264\ a_0$ ($CeCoIn_5$), $a = 8.791\ a_0$ and $c = 14.252\ a_0$ ($CeRhIn_5$), and $a = 8.818\ a_0$ and $c = 14.205\ a_0$ ($CeIrIn_5$). For the one special In-position we also adopted the experimental values.

The band structure of $CeCoIn_5$ computed with the fully relativistic scheme is presented in Fig. 1. The band structure of $CeCoIn_5$ obtained with the scalar-relativistic scheme, as well as the band structures of nonmagnetic $CeRhIn_5$ and $CeIrIn_5$ are only slightly different and therefore not presented here. We find for each of the Ce-115 systems using either the scalar-relativistic or fully relativistic scheme three bands which cross the Fermi surface. These bands are denoted as Band 131, Band 133 and Band 135, according to their number in the valence band complex of the fully relativistic calculation counted from below. Following the line $\Gamma - M$ in Fig. 1 the crossing points of Bands 131, 133 and 135 (in that order) with the Fermi level are clearly visible. The influence of relativistic effects is most pronounced along the $\Gamma - Z$ line, where the upper two bands 133 and 135 remain degenerate in the scalar-relativistic calculation. However, the fully relativistic effect along $\Gamma - Z$ and at other places in the Brillouin zone (BZ) have only minor influence on the Fermi surface. We find only small differences in the extremal Fermi surface cross sections which will be discussed in the next Section.

Also, the differences in the band structures calculated for the three compounds $CeCoIn_5$, $CeRhIn_5$, and $CeIrIn_5$ are small. For example, in the fully relativistic calculation of $CeRhIn_5$, band number 133 does not cross the Fermi level between A and R in variance to Fig. 1, where it just crosses the Fermi level. As a result, the two extremal orbits (for $H \parallel c$) of band 133 which are centered around the A point for $CeCoIn_5$ are no longer closed orbits for $CeRhIn_5$. Instead, one finds for $CeRhIn_5$ corresponding orbits which are closed around other points in k-space, however.

$CeRhIn_5$ differs in its physical properties from the other two compounds and a debate concerning the localization of the Ce $4f$ electron has emerged.[10,11,15] Below we will see that the agreement between calculated and measured dHvA frequencies is indeed significantly worse for $CeRhIn_5$ (in comparison to the Co- and Ir-

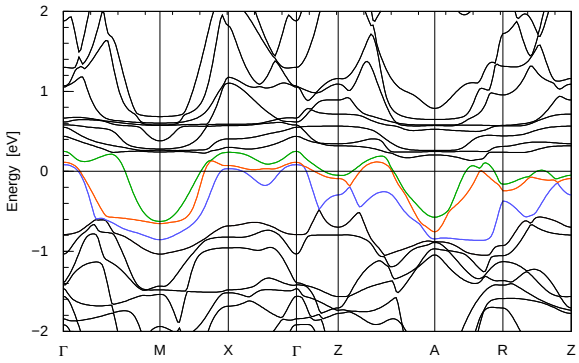

FIG. 1: (Color online) The energy bands of nonmagnetic $CeCoIn_5$ calculated using the fully relativistic FPLO method. The bands 131, 133, and 135 that cut the Fermi energy are highlighted by the colors.

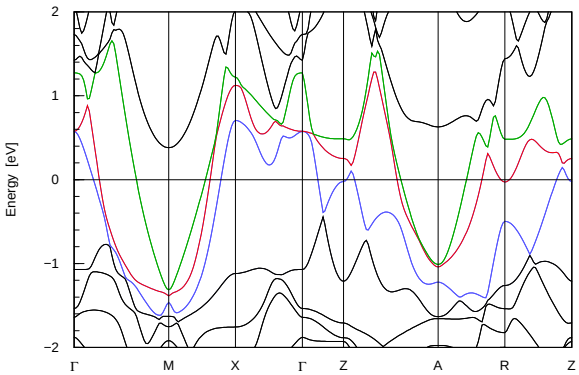

FIG. 2: (Color online) The energy bands of $CeRhIn_5$ calculated with the Ce $4f$ electron treated as a core electron. The important bands $131 - 135$ are colored as in Fig. 1.

compounds) if we treat the Ce $4f$ electrons itinerantly. Therefore, we present in Fig. 2 the result of a fully relativistic band-structure calculation for $CeRhIn_5$, where its Ce $4f$ electron was treated as a core electron ($4f$-c scheme). By comparison with Fig. 1 one can easily conclude that the seven, nearly dispersionless bands in Fig. 1, situated at about 0.5 eV are of Ce $4f$ character. These bands are especially clearly visible above the Fermi level at A and M, but they are mixed with other bands elsewhere and the lowest one drops below the Fermi level between Γ and X. By calculating additionally the atomic character within each band (not shown) we have found that the bands which cross the Fermi level in Fig. 1 have a considerable f character as well. Especially pronounced is the f character at the Fermi energy between X and Γ, as well as between R and Z. Considerable f character below the Fermi energy exists only at the high-symmetry points Z and R. Other states which contribute significantly at the Fermi energy are the In $5p$ orbitals. This is especially true for the bands centered around the A and M points. If we compare the energy bands in Figs. 1 and 2 between M and Γ, or between M and X, we find in both cases three bands crossing the Fermi energy. The two upper bands (bands 133 and 135 in the fully relativistic case) give rise to closed orbits centered at M which are of predominantly In $5p$ character and present at E_F irrespective of the treatment of the Ce $4f$ electrons. However, the areas are different. The same is true for the two, electron-like bands, centered around the A point. In the present study, we did not try to interpret the dHvA data of $CeRhIn_5$ with a band-structure calculation taking into account the correct low-temperature antiferromagnetic order of that compound.

Let us shortly compare our band-structure results with those published already in the literature. We find that our FPLO result agrees best with the FLAPW band structure[14] published for $CeIrIn_5$. This agreement concerns also the corresponding Fermi surfaces and, for $CeCoIn_5$ it holds as well (see Refs. 13 and 15). The relativistic linear augmented-plane-wave (RLAPW) calculations published in Ref. 19 show in contrast to our results a fourth band crossing the Fermi surface. The corresponding band in our calculation can be seen in Fig. 2 at about 0.4 eV *above* E_F at the M point and it consists mainly of In $5p$ character. It could drop below the Fermi level due to the use of a non-optimal basis set. The nonrelativistic band structure of $CeCoIn_5$ published in Ref. 18 shows a rough agreement with our results with respect to the band characters, but considerable differences due to relativistic effects exist near E_F. For instance, due to the lack of spin-orbit splitting, the $4f$ band complex is much narrower there.[18] Finally, band-structure results and the corresponding Fermi surface of $CeRhIn_5$ were reported in Ref. 10. Whereas the band structure is quite similar to our results, there exist some differences in the calculated dHvA data as well as in the assignment of the measured dHvA frequencies.

IV. EXTREMAL ORBITS

Based on the band-structure results, we calculated the dHvA frequencies and effective masses for all extremal orbits with $H \parallel c$. The most relevant calculations were performed in the fully relativistic scheme for which a complete analysis has been performed and which are compared with the scalar-relativistic calculations. The individual extremal orbits were already shown in Fig. 5 of Ref. 14 (see also Refs. 13 and 15) which we therefore not repeated here. For clarity sake we also use the same notation[14] except for one minor modification: in some cases the orbit a does not exist and is broken into two other orbits which we then denote as a_1 and a_2. The band numbers in Tables I–III refer to the valence bands in the fully relativistic scheme counted from below as introduced in the previous Section. In the case of $CeRhIn_5$ we present also some dHvA data for the most prominent Fermi surface sheets which we calculated using the $4f$-c scheme. We did, however, not attempt to identify all the experimentally observed orbits. Lastly, we note that some orbits in either the scalar- or fully relativistic scheme are not presented because they do not exist as a

closed, extremal orbit.

TABLE I: Calculated dHvA frequencies F (in kT) and effective masses m (in m_0) for $CeCoIn_5$ with $H \parallel c$. The calculations were performed treating the Ce $4f$ electrons as delocalized and adopting either the scalar-relativistic or the fully relativistic approach. The notation of the extremal orbits can be found in Ref. 14.

	central	band	F (kT)		m (m_0)	
symbol	point	no.	sc-rel.	rel.	sc-rel.	rel.
g	Γ	131	0.809	0.761	-0.661	-0.814
h	X	131	0.460	0.438	-0.669	-0.974
β_1	M	133	12.910	12.680	2.279	2.314
β_2	A	133	6.312	6.295	1.232	1.474
c	A	133	13.496	13.113	-3.178	-3.645
α_1	$A'_{k_z=0.18}$	135	5.399	5.352	1.543	1.621
α_2	M	135	4.599	4.475	0.977	0.996
α_3	A	135	4.069	4.060	1.155	1.317
a_1	Z	135	1.280	1.264	1.445	1.536
a_2	R	135	1.186	1.136	0.909	0.946

TABLE II: Calculated dHvA frequencies F and effective masses m for $H \parallel c$ in $CeIrIn_5$.

	central	band	F (kT)		m (m_0)	
symbol	point	no.	sc-rel.	rel.	sc-rel.	rel.
g	Γ	131	0.701	0.678	-0.566	-0.632
h	X	131	0.137	0.224	-0.776	-0.693
β_1	M	133	12.086	12.106	1.957	2.226
β_2	A	133	6.083	5.963	1.062	1.156
c	A	133	13.175	12.772	-2.860	-3.386
α_1	$A'_{k_z=0.18}$	135	4.994	4.984	1.387	1.694
α_2	M	135	4.148	4.017	0.929	1.026
α_3	A	135	3.877	3.929	0.998	1.324
a_1	Z	135	1.418	open	1.903	open
a_2	R	135	1.262	open	1.150	open
a	A	135	open	15.011	open	-4.527

Let us now characterize the various extremal orbits in more detail. **Band 131** gives rise to two small orbits around Γ (orbit g) and around X (orbit h). These two orbits are hole-like and they are present in all three compounds. **Band 133** creates the electron-like orbit β_1 around M, and also two orbits, β_2 and c, around the A point which are electron- and hole-like, respectively. The two distinct kinds of orbits around A may be understood from the band structure (Fig. 1), since Band 133 crosses the Fermi level twice along each of the high-symmetry directions $A-R$ and $A-Z$, respectively.

The most important orbits are α_1, α_2 and α_3, which are connected with **Band 135**. These orbits are the ones that are most clearly visible in experiment[15,16,17] (together with β_2) and, in addition, they were observed in all three compounds. They correspond to a cylindrical Fermi surface sheet along the $M-A$ axis in the BZ. Orbit α_3 is centered around the A point, orbit α_2 around M point, and orbit α_1 is centered around a point in between A and M. These three orbits are all electron-like. The hole-like orbit a around point A in k-space exists only in the fully relativistic calculation of $CeIrIn_5$. In all other cases it breaks up into two orbits (for which we introduced the notations a_1 and a_2) which are centered around Z and R, respectively, and which are electron-like.

To explain the peculiarities of the three compounds summarized in Tables I–III some comments are given in the following:

- In the case of $CeRhIn_5$ (Table III), the orbit β_2 is an extremal orbit around the A point in the scalar-relativistic scheme as well as in the $4f$-c scheme. In the fully relativistic case, the corresponding orbit β_2 has an extremal cross section at $k_z = 0.25$ (denoted by A') and it disappears for larger values of k_z including the A point.

- For $CeRhIn_5$ (Table III), the extremal orbit c is centered around A in the scalar-relativistic scheme, but has an extremal cross section around A' with $k_z = 0.27$ in the fully relativistic case.

- In the $4f$-c scheme (only relevant for $CeRhIn_5$, Table III) one can find more extremal orbits than given in the Table. Only those extremal orbits are presented which have a clear correspondence in the fully relativistic scheme. Also, there are extremal orbits in the fully relativistic calculation which have no correspondence in the $4f$-c scheme.

- As was already noted, the orbit a exists only in the fully relativistic calculation for $CeIrIn_5$ (Table II) but breaks up into two orbits a_1 and a_2 in the scalar-relativistic calculation for that compound as well as for the other Ce-115 compounds.

V. DISCUSSION AND COMPARISON

In Table IV we compare our calculated dHvA frequencies for **$CeCoIn_5$** to the available experimental data. Our values—calculated assuming delocalized $4f$'s—agree very well with the theoretical results reported by Settai *et al.*[13] (who give, however, not all frequencies that exist). The two published experimental data sets[12,13] agree reasonably well with one another, too, and with the theoretical values. The experimental data of both groups[12,13] complete each other to some extent. Taking all results together, only orbits c, a_1, and a_2 were never observed. It might be that orbit a is not split in reality and, consequently, it should be expected at a high frequency. In general it is increasingly difficult to detect high frequency orbits with good precision. This difficulty of the dHvA technique could also be the reason why orbit c has not been detected.

The situation is similar for **$CeIrIn_5$** (see Table V). The agreement of our data with the FLAPW results[14] is excellent. The correspondence with the experimental

TABLE III: De Haas-van Alphen frequencies F and effective masses m calculated for $CeRhIn_5$ with $H \parallel c$. The presented dHvA quantities were calculated treating the Ce $4f$ electrons as delocalized, adopting either the scalar-relativistic or the fully relativistic scheme, as well as with the $4f$-c scheme, in which the Ce $4f$ electron is treated as localized.

	central	band	F (kT)			m (m_0)		
symbol	point	no.	sc-rel.	rel.	$4f$-c	sc-rel.	rel.	$4f$-c
g	Γ	131	0.848	0.821		-0.645	-0.807	
h	X	131	0.544	0.537		-0.666	-0.899	
β_1	M	133	12.759	12.201	10.250	2.007	1.994	0.629
β_2	A	133	5.808	open	6.073	1.080	open	0.551
β_2	$A'_{k_z=0.25}$	133		6.534			1.484	
c	A	133	12.976	open		-2.707	open	
c	$A'_{k_z=0.27}$	133		15.684			-5.970	
α_1	$A'_{k_z=0.19}$	135		5.383	4.567		1.535	0.549
α_2	M	135	4.371	4.213	3.928	0.894	0.952	0.467
α_3	A	135	4.052	3.899	3.483	0.997	1.203	0.472
a_1	Z	135	1.414	1.312		1.310	1.524	
a_2	R	135	1.140	1.051		0.836	0.955	

TABLE IV: Comparison of several experimental and theoretical dHvA frequencies F (in kT) for $CeCoIn_5$.

symbol	symbol	theory F		experiment F	
Refs. 13,14	Ref. 12	present	Ref. 13	Ref. 12	Ref. 13
c		13.11	13.30		
β_1		12.68	13.00		12.00
β_2	F_6	6.30	6.45	7.535	7.50
α_1	F_5	5.35	5.43	5.401	5.56
α_2	F_4	4.48	4.53	5.161	4.53
α_3	F_3	4.06	3.90	4.566	4.24
a_1		1.26			
a_2		1.14			
g	F_2	0.76		0.411	
h	F_1	0.44		0.267	

TABLE V: Comparison of experimental and theoretical dHvA frequencies and masses of $CeIrIn_5$.

symbol	theory F		exp. F	theory m		exp. m
Ref. 14	present	Ref. 14	Ref. 14	present	Ref. 14	Ref. 14
a	15.01	15.20		4.53	4.89	
c	12.77	12.80		3.39	3.95	
β_1	12.11	12.40	12.00	2.23	3.32	32
β_2	5.96	6.18	6.11-6.59	1.16	1.33	21-30
α_1	4.98	5.00	5.07-5.56	1.69	1.89	17-25
α_2	4.02	4.03	4.53	1.03	1.15	29
α_3	3.93	3.65	4.24	1.32	1.37	10
g	0.68	0.70		0.63	0.64	
h	0.22	0.14	0.27	0.69	1.04	6.3

data is also gratifying. Nearly all the predicted orbits were experimentally observed. Only the orbits g, a, and c are missing. The later ones belong to the more difficult to detect high-frequency orbits, but g is a low-frequency orbit. It could be that experimentally the two orbits g and h could not be separated or that the intensity of g was too low. The orbits β_2 and α_1 displayed some splitting in the experiment.[14] Despite the good agreement achieved for the dHvA frequencies, the experimental cyclotron masses are extremely enhanced compared to the calculated (unehanced) orbital masses. This experimental observation understandably reflects the heavy fermion behavior of $CeIrIn_5$, which has a specific heat coefficient[2] of about 750 mJ/molK^2. A similar mass enhancement exists for $CeCoIn_5$ (see Ref. 13). The mass enhancement is connected with the $4f$ character of the bands.

The compound **$CeRhIn_5$** exhibits a remarkably different behavior. The dHvA experiments performed in the antiferromagnetic state[10,15] detected a multitude of low-frequency branches besides the main branches β_2, α_1 and $\alpha_{2,3}$. Here, our focus is not to describe this multitude of low-frequency orbits, for which most probably the correct antiferromagnetically ordered structure has to be taken into account in the band-structure calculation. In addition, in the existing experiments only the main branches could be unambiguously assigned.[15] In Table VI we therefore compare only the experimental and theoretical results for these main branches.

TABLE VI: Comparison of theoretical and experimental results for the dominating dHvA frequencies in $CeRhIn_5$. In our calculations (denoted 'present') the Ce $4f$ electrons are treated either as delocalized ($4f$-val.) or localized ($4f$-c).

		theory F (kT)			exp. F (kT)		
symbol	symbol	present					
a	b	$4f$-val.	$4f$-c	b	a	b	c
β_2	F'_8	6.53	6.07	6.878	6.13	6.12	6.256
α_1		5.38	4.57	5.562	4.67		4.686
α_2	F'_7	4.21	3.93	4.331	3.67	3.60	3.605
α_3	F'_7	3.90	3.48	3.951	3.67	3.60	3.605

a: Ref. 15; b: Ref. 10; c: Ref. 9.

If we would start our interpretation of the dHvA frequencies in $CeRhIn_5$ with treating the Ce $4f$ electrons as

valence electrons in the fully relativistic scheme, then we immediately observe an important difference with regard to both $CeCoIn_5$ and $CeIrIn_5$: whereas the experimental data are slightly larger (up to 10 percent) than the theoretical values for the later two superconducting compounds, they are up to 10 percent *smaller* for $CeRhIn_5$. In contrast, the results obtained with the $4f$-c scheme fit much better in the general chemical trend. Since there is no $4f$ contribution at the Fermi level the volume enclosed by the Fermi surface shrinks and so does, consequently, the corresponding areas of extremal orbits. As a result the theoretical values are now *smaller* than the measured ones in accordance with the general trend in the series $CeMIn_5$. It should be noted, however, that the absolute deviation from the experimental values is not significantly improved.

What concerns the effective masses, these are enhanced in $CeRhIn_5$ as well, but only moderately. The experimental value for the mass m/m_0 of orbit β_2 is 6.1 ± 0.3 (Ref. 10) or 6.5 ± 0.8 (Ref. 9), respectively, whereas theoretically it was found to be 1.48 (in the fully relativistic scheme) or 0.55 (in the $4f$-c scheme), see Table III). The corresponding values for orbit α_2 are: experiment: 4.6 ± 1.0 (Ref. 10) or 4.8 ± 0.4 (Ref. 9), and theory: 0.95 (rel.) or 0.47 ($4f$-c). Although the inclusion of $4f$ orbitals into the valence-band complex enhances the effective masses even in LSDA, that does not necessarily advocate delocalized $4f$'s. Instead, it can be expected that the dominating mass enhancement in $CeRhIn_5$ occurs because of a strong interaction between conduction electrons and magnetic fluctuations, which is not taken into account in our calculation, however. Under pressure the antiferromagnetic order disappears in $CeRhIn_5$ yet the spin fluctuations and their interaction with the conduction electrons intensify, as suggested by the pronounced increase observed for the effective dHvA masses.[16,17]

To confirm our interpretation of localized $4f$ behavior, we calculated in addition the angular dependence of the dHvA frequencies of the main branches treating the $4f$ electrons as core states. The results are shown in Fig. 3. As can be seen, the characteristic angular dependence of the various branches is well reproduced. The calculated splitting of the α_2 and α_3 branches is larger than the experimentally observed splitting, the reason why remains an open question at the moment. The related compound $LaRhIn_5$ displayed also a larger $\alpha_2 - \alpha_3$ splitting.[15] If we would have displayed the results calculated treating the $4f$ electrons as itinerant, then the theoretical branches would lie much higher than the experimental ones and the agreement would be much worse. Thus, our calculations support the picture of reasonably localized $4f$ behavior in $CeRhIn_5$, at variance with the much more delocalized $4f$ behavior in $CeCoIn_5$ and $CeIrIn_5$. In Fig. 3 one can also see the multitude of low-frequency orbits, the origin of which could be resolved only by band-structure calculations taking the antiferromagnetic ordering into account.

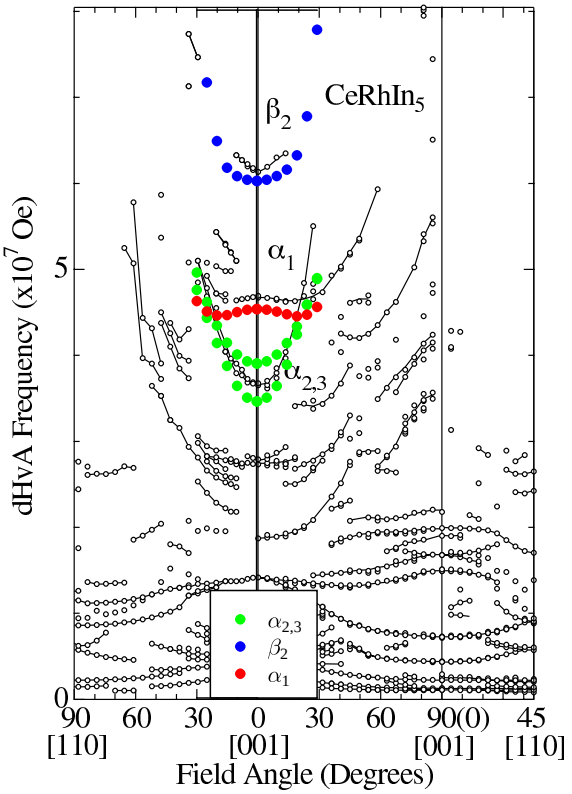

FIG. 3: (Color online) Measured angular dependence of dHvA frequencies in $CeRhIn_5$ (open points, from Ref. 15) in comparison to the theoretical ones, calculated with the fully relativistic FPLO scheme and treating the Ce $4f$ electron as core electron (filled symbols).

VI. CONCLUSIONS

Our investigation of the electronic structures and dHvA quantum oscillations in the Ce-115 corroborate the following picture of these materials. In $CeCoIn_5$ and $CeIrIn_5$ the Ce $4f$ electrons appear to be rather delocalized. Therefore, treating the $4f$ electrons in these two compounds like itinerant states we do obtain a good description of the measured dHvA frequencies. However, the experimental effective masses of the extremal orbits are considerably enhanced over the band-structure effective masses. In spite of the substantial many-particle enhancement of the masses in the proximity of the heavy fermion state, it is surprisingly how well the Fermi surface cross sections are described by the band-structure calculations.

The behavior of $CeRhIn_5$ differs from that of $CeCoIn_5$ and $CeIrIn_5$. In order to provide an explanation of the main dHvA branches of $CeRhIn_5$, taking into account also the chemical trend in the series $CeCoIn_5$–$CeIrIn_5$, we find that it is better to treat the Ce $4f$ electrons as localized. This finding is in agreement with some of

the observed differences between the Rh-compound and the Co- and Ir-compounds, as, e.g., the lower specific heat and the antiferromagnetic order of the Rh-115 compound. The antiferromagnetic structure leads additionally to a multitude of low-frequency dHvA branches that are not detected for the other two compounds, an explanation of which would require a careful study of the Fermi surface of the antiferromagnetically ordered compound.

The mass enhancement observed within the Ce-115 series is most likely due to spin fluctuations as well as charge fluctuations, but it comes about in a different manner for $CeRhIn_5$. The moderate enhancement of the latter Ce-115 compound occurs due to spin fluctuations on top of the 'frozen' magnetic state. The appreciable mass enhancement in $CeCoIn_5$ and $CeIrIn_5$, on the contrary, seems to be related to the more itinerant $4f$ electrons, which have a substantial weight near the Fermi energy and, in addition to being responsible for the fluctuating spin polarization, charge fluctuations of the $4f$'s can now contribute to the mass enhancement, also.

Another mystery is why the deviating behavior occurs for the Rh-compound and not, for example, for the Ir-compound. It was noted earlier that small changes in the lattice parameters of the Rh-compound do already lead to a physical behavior very similar to that of $CeCoIn_5$ and $CeIrIn_5$,[1] but this does not provide a microscopic explanation. The small Néel temperature of $CeRhIn_5$ ($T_N = 3.8$ K) suggests that all three compounds could be close to antiferromagnetic ordering. This gives an indication of what the pairing mechanism of the unconventional superconductivity[6,7,8] could be. Most likely significant antiferromagnetic spin fluctuations are present in all three compounds at low temperatures, the strength of which depends delicately on the Ce-interplane distance (i.e., the c/a ratio). The c/a ratio apparently also has a pronounced influence on the localization degree of the Ce $4f$ states. If the antiferromagnetic interaction is not strong enough to achieve antiferromagnetic ordering the next favorable order parameter is superconductivity, which might still benefit from the antiferromagnetic fluctuations present. The fact that the superconducting order parameter has unconventional $d_{x^2-y^2}$-symmetry[7] might also correspond to an unconventional pairing mechanism, however, it has been shown that this must not always automatically be so.[25]

The discussion of the origin of the unconventional superconductivity also touches upon the importance of relativistic effects, as claimed in Ref. 19. In the later work, substantial differences between the Fermi surfaces computed with the scalar- and fully relativistic approximations were reported. In contrast, we find in our investigation that the results of the scalar- and fully relativistic schemes are very similar for all the Ce-115 compounds. In particular, no fourth band crossing the Fermi level is found. Therefore, there is apparently not a compulsory reason for a fully relativistic description of the superconductivity in the Ce-115 compounds.

Acknowledgments

This work was supported financially by the Egyptian Ministry of Higher Education and Scientific Research and by the German Sonderforschungsbereich 463, Dresden.

[1] H. Hegger, C. Petrovic, E. G. Moshopoulou, M. F. Hundley, J. L. Sarrao, Z. Fisk, and J. D. Thompson, Phys. Rev. Lett. **84**, 4986 (2000).
[2] C. Petrovic, R. Movshovich, M. Jaime, P. G. Pagliuso, M. F. Hundley, J. L. Sarrao, Z. Fisk, and J. D. Thompson, Europhys. Lett. **53**, 354 (2001).
[3] C. Petrovic, P. G. Pagliuso, M. F. Hundley, R. Movshovich, J. L. Sarrao, J. D. Thompson, Z. Fisk, and P. Monthoux, J. Phys. Condens. Matter **13**, L337 (2001).
[4] Wei Bao, P. G. Pagliuso, J. L. Sarrao, J. D. Thompson, Z. Fisk, J. W. Lynn, and R. W. Erwin, Phys. Rev. B **62**, R14621 (2000).
[5] G.-Q. Zheng, K. Tanabe, T. Mito, S. Kawasaki, Y. Kitaoka, D. Aoki, Y. Haga, and Y. Ōnuki, Phys. Rev. Lett. **86**, 4664 (2001).
[6] R. Movshovich, M. Jaime, J. D. Thompson, C. Petrovic, Z. Fisk, P. G. Pagliuso, and J. L. Sarrao, Phys. Rev. Lett. **86**, 5152 (2001).
[7] K. Izawa, H. Yamaguchi, Y. Matsuda, H. Shishido, R. Settai, and Y. Ōnuki, Phys. Rev. Lett. **87**, 057002 (2001).
[8] R. J. Ormeno, A. Sibley, C. E. Gough, S. Sebastian, and I. R. Fisher, Phys. Rev. Lett. **88**, 047005 (2002).
[9] A. L. Cornelius, A. J. Arko, J. L. Sarrao, and N. Harrison, Phys. Rev. B **62**, 14181 (2000).
[10] D. Hall, E. C. Palm, T. P. Murphy, S. W. Tozer, E. Miller-Ricci, L. Peabody, C. Quay Huei Li, U. Alver, R. G. Goodrich, J. L. Sarrao, P. G. Pagliuso, J. M. Wills, and Z. Fisk, Phys. Rev. B **64**, 064506 (2001).
[11] U. Alver, R. G. Goodrich, N. Harrison, D. W. Hall, E. C. Palm, T. P. Murphy, S. W. Tozer, P. G. Pagliuso, N. O. Moreno, J. L. Sarrao, and Z. Fisk, Phys. Rev. **64**, 180402(R) (2001).
[12] D. Hall, E. C. Palm, T. P. Murphy, S. W. Tozer, Z. Fisk, U. Alver, R. G. Goodrich, J. L. Sarrao, P. G. Pagliuso, and T. Ebihara, Phys. Rev. B **64**, 212508 (2001).
[13] R. Settai, H. Shishido, S. Ikeda, Y. Murakawa, M. Nakashima, D. Aoki, Y. Haga, H. Harima, and Y. Ōnuki, J. Phys.: Condens. Matter **13**, L627 (2001).
[14] Y. Haga, Y. Inada, H. Harima, K. Oikawa, M. Murakawa, H. Nakawaki, Y. Tokiwa, D. Aoki, H. Shishido, S. Ikead, N. Watanabe, and Y. Ōnuki, Phys. Rev. B **63**, 060503(R) (2001).
[15] H. Shishido, R. Settai, D. Aoki, S. Ikeda, H. Nakawaki, N. Nakamura, T. Iizuka, Y. Inada, K. Sugiyama, T. Takeuchi, K. Kindo, T. C. Kobayasi, Y. Haga, H. Harima, Y. Aoki, T. Namiki, H. Sato, and Y. Ōnuki , J. Phys. Soc. Jpn. **71**, 162 (2002).
[16] H. Shishido, R. Settai, S. Araki, T. Ueda, Y. Inada, T. C.

Kobayashi, T. Muramatsu, Y. Haga, and Y. Ōnuki, Phys. Rev. B **66**, 214510 (2002).
[17] H. Shishido, R. Settai, S. Araki, T. Ueda, Y. Inada, H. Harima, and Y. Ōnuki, Physica B **329–333**, 526 (2003).
[18] J. Costa-Quintana and F. Lopéz-Aguilar, Phys. Rev. B **67**, 132507 (2003).
[19] T. Maehira, T. Hotta, K. Ueda, and A. Hasegawa, J. Phys. Soc. Jpn. **72**, 854 (2003).
[20] T. Hotta and K. Ueda, Phys. Rev. B **67**, 104518 (2003).
[21] K. Koepernik and H. Eschrig, Phys. Rev. B **59**, 1743 (1999).
[22] I. Opahle, PhD thesis, University of Technology Dresden, 2001.
[23] J. P. Perdew and Y. Wang, Phys. Rev. B **45**, 13244 (1992).
[24] P. M. Oppeneer and A. Lodder, J. Phys. F: Metal Phys. **17** 1901 (1987).
[25] P. M. Oppeneer and G. Varelogiannis, Phys. Rev. B **68**, 214512 (2003).